Obtaining the frequencies of Schenberg detector sphere using finite element modelling

F S Bortoli[1], R N Duarte[1] ,R C Souza[1] , N S Magalhaes[2], C Frajuca[3] and S T Sousa[4]

[1] Federal Institute of Education, Science and Technology of Sao Paulo
Rua Pedro Vicente, 625, Caninde – Sao Paulo – SP – Brazil BR
CEP: 01109-010 www.ifsp.edu.br
[2] Physics Department - Federal University of Sao Paulo
Diadema - SP - Brazil
[3] IMEF Institute - Federal University of Rio Grande
Rio Grande - RS - Brazil
[4] FATEC ITAQUERA - FATEC
São Paulo - SP - Brazil

E-mail: frajuca@gmail.com

Abstract: The resonant-mass gravitational wave detector SCHENBERG is a spherical detector that operates with a central frequency close to 3200 Hz and a bandwidth around 200 Hz. It has a spherical mass that works as an antenna whose weight is 1150 kg and is connected to the outer environment by a suspension system designed to attenuate local noise due to seism as well as other sources; the sphere is suspended by its center of mass. When a gravitational wave passes by the detector, the antenna is expected to vibrate. This motion should be monitored by six parametric microwave transducers whose output signals will be digitally analyzed. In order to determine the detector performance better, it is necessary to obtain the vibration frequencies of the sphere with a better precision. To achieve such a goal the sphere with the holes to mount the transducers and the central hole from which the sphere is suspended is simulated in a finite element method program when the gravity is applied to the sphere and the deformation is kept. After that the vibration normal modes of the sphere are calculated and they are compared to the experimental results.

1. Introduction

Some of the authors are members of the GRAVITON Group, a Brazilian group dedicated to the study of gravity, which has gravitational waves as its main research area of investigation. GRAVITON group efforts toward the understanding of gravity can be summarized in references [1-27].

Among the main parameters of a gravitational wave resonant-mass detector are its frequencies and operating band. And although the Schenberg detector antenna is spherical, a well-studied geometry, its construction required changes that made it no longer a perfect sphere. Therefore, the way to study and evaluate those parameters is no longer analytical and now it is done through simulations, in this case by finite element modeling (FEM). In this approach, several sets of definitions are possible that affect the results obtained and the simulation time used. In previous works [14, 15, 17, 20, 21, 23, 24, 25, 27], results were obtained that considered the system detached from the external environment and without the existence of gravity, choices that significantly reduce the computation processing time in the simulation. In this work, these definitions were changed, now taking into consideration both gravity and the existence of a constraint located in the same place where the Schenberg suspension is connected [23]. It was necessary to confirm the assumption that these factors affect very little the parameters evaluated here, and also how they would. Thus, in this work it was possible to observe the changes in the frequency and working band parameters obtained with this new approach.

2. Schenberg detector

Schenberg has a solid spherical antenna made with an alloy of Cu (94%) and Al (6%), with a mass of 1,150 Kg. In addition to having 9 holes located on its surface for fixing the transducers, according to a distribution based on a truncated icosahedron [28], it also has a central hole for its support and connection with the suspension of the sphere. This central hole contains in its center a conical surface that receives the rod that connects the sphere to its suspension. The schematics of the Schenberg detector can be seen in figure 1. Among other aspects, the figure shows the suspension of the sphere with 6 disk-like devices (with approximately 120 kg each), 4 of which are made with the same material as the sphere and the 2 lower discs made of copper. At the top of this suspension, an upper rod connects it to a tire which, in turn, is connected to a mass of approximately 4 metric tons. This entire assembly involving the suspension, tire and upper platform was designed to attenuate local seismic noise, as well as other noise within the Schenberg's detection band.

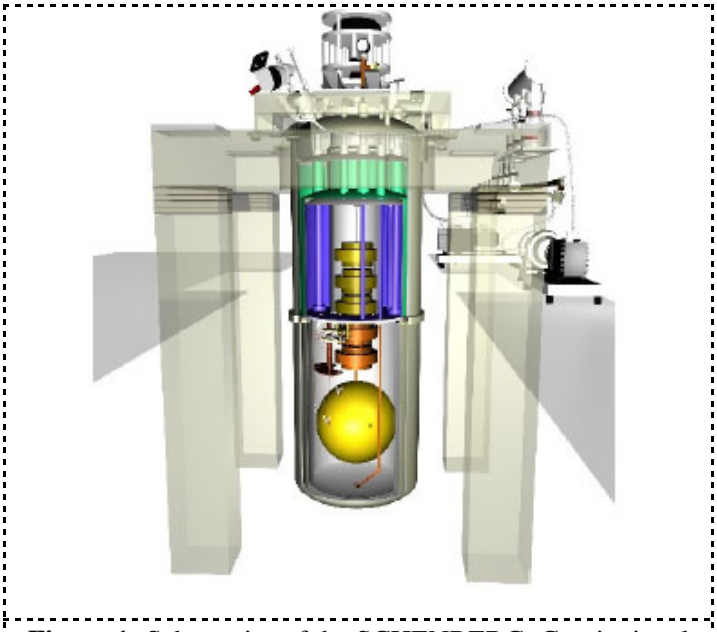

Figure 1: Schematics of the SCHENBERG Gravitational Wave Detector (Credit: Xavier P. M. Gratens).

The set involving the sphere, its suspension, in addition to other devices of the cryogenics system and electronic signal processing, are packaged inside a dewar. This, in turn, contains nitrogen and helium and its function is to produce the cryogenic cooling necessary to reduce the vibrations from the Brownian noise produced by this whole set.

3. Displacement and deformation under gravity

The study of the effect of gravity on the detection frequencies of the Schenberg detector started with the analysis of the static effect of gravity on the displacements of its massive sphere. Thus, the starting point was to carry out simulations of the sphere using FEM, considering it connected to an inertial system in the same region where its suspension was connected. In these analyses, models of the sphere were built and, using the experience accumulated previously, static simulations of this system were carried out. Figure 2 shows the model of this massive sphere, 65 cm in diameter, containing the holes for fixing the transducers and the central hole where the region of contact and connection of the sphere with its suspension is located.

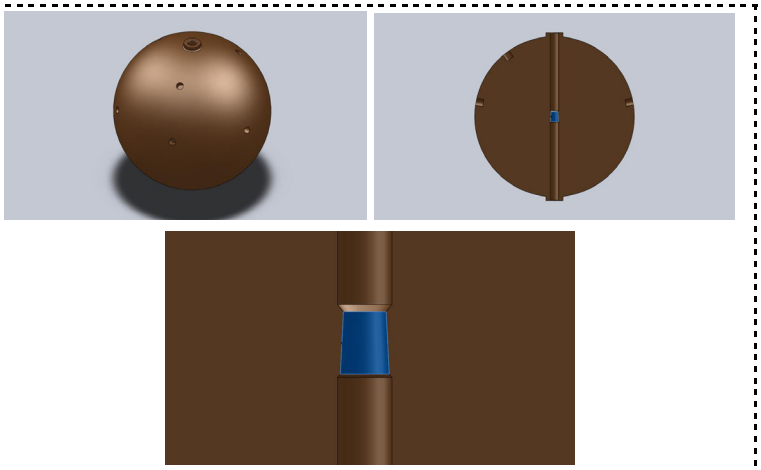

Figure 2: Massive sphere model of the Schenberg detector used in static simulation and in obtaining normal frequency modes. The figures show the upper and lower flanges, the holes for fixing the transducers, the central hole and the region of this hole used to connect the sphere to its suspension. The lower image shows in detail this region used to connect the sphere. Source: The authors.

From the simulation results it was possible to evaluate the effect of gravity on the displacements resulting from the deformation of the sphere due to its own weight. Figure 3 shows the results of these displacements without distinguishing their directions, highlighting the surfaces on which these displacements had the same magnitude.

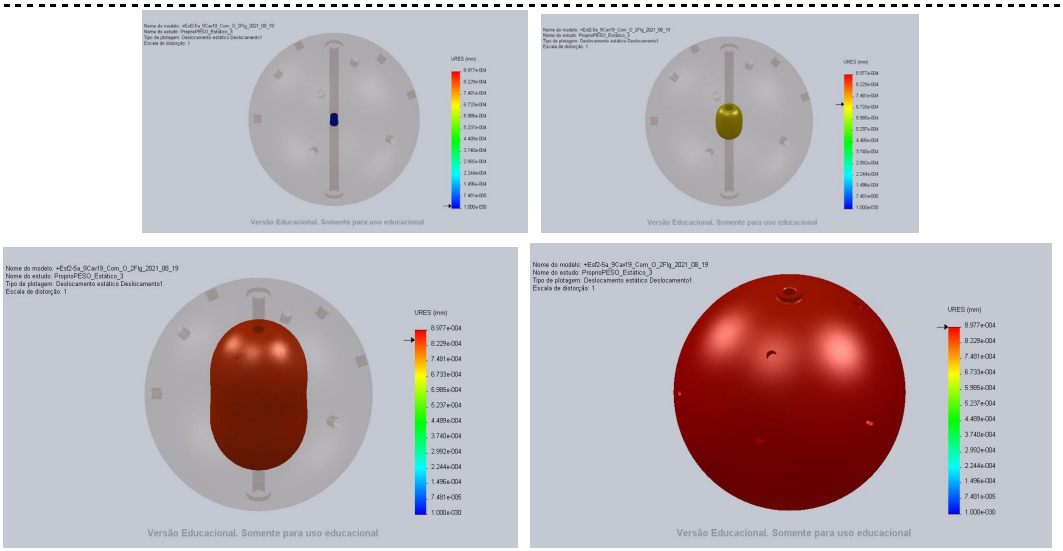

Figure 3: Some of the results of static simulation by FEM of the detector's massive sphere. Each image shows a surface within the sphere where the displacements had the same magnitude. The results do not distinguish the direction of the displacements, only their magnitude. Source: The authors.

The greatest absolute displacements occurred in the region corresponding to the sphere's equator and were more intense in the regions close to the sphere's surface.

Another way to indicate displacements on the sphere is to use a vector plot. Figure 4 shows the vector plot referring to the simulation performed, where it is possible to observe the direction of displacements in the various regions of the sphere.

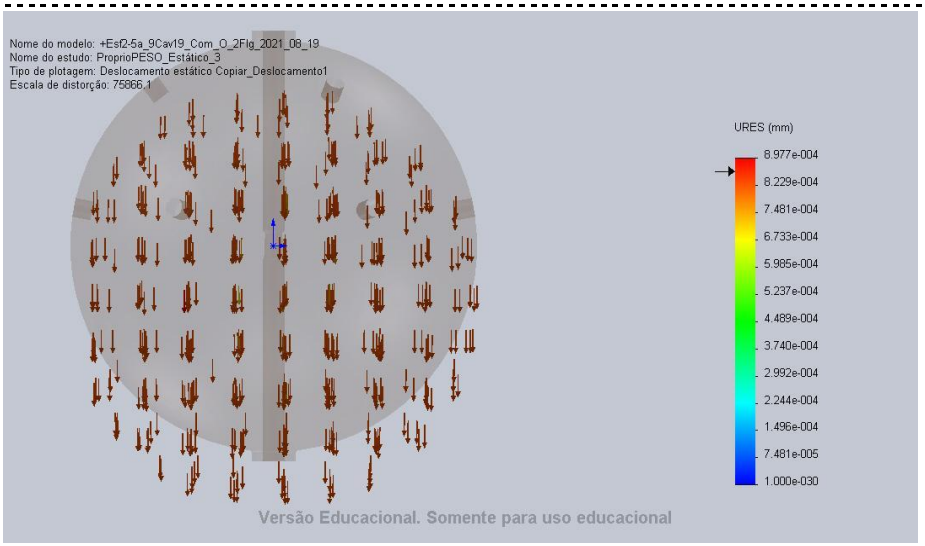

Figure 4: Vector plot referring to the simulation performed. It is possible to observe the direction of displacements in the various regions of the sphere. Source: From the authors.

4. Stress under gravity

As a result of the static simulation using FEM, it was also possible to analyze the behavior of the stress distribution in the detector's massive sphere. More precisely, changes in von Mises stress were analyzed. Due to the characteristics of von Mises stresses, these results do not indicate whether they are tensile or compressive stresses.

Figure 5 shows some of the results for the von Mises stress, highlighting the surfaces within the sphere where these stresses had the same magnitude.

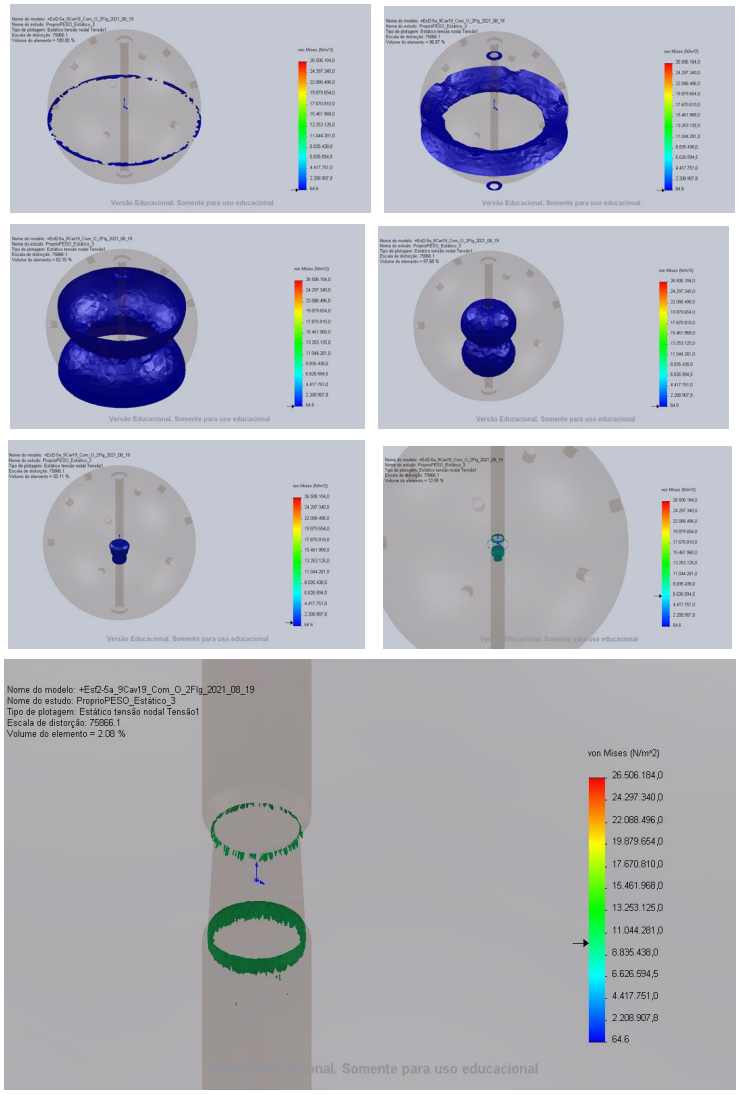

Figure 5: Some of the results of static simulation by FEM for the von Mises stress on the detector's massive sphere. Each image shows a surface within the sphere where the von Mises stress were of the same magnitude. This type of study does not distinguish whether they are tensile or compression stresses. The lower image shows in detail the region used to connect the sphere. Source: From the authors.

The images in figure 5 indicate that the values of von Mises stress are higher in the region where the connection of the sphere with the suspension is made. On the other surfaces, where stresses occur due to their own weight, there will be both tensile stresses (predominantly above the sphere's equator) as well as compression stresses (in the region below the sphere's equator), which are not available in this type of study.

5. Frequencies

The massive sphere model used in this stage of the work also has the transducer fixing holes, the central hole with the suspension connection and the upper and lower flanges. In this model, the sphere was also constrained in the same region in which its suspension is connected and was subjected to the action of gravity. With these configurations a new simulation was made to obtain the sphere frequencies. Taking into account the interest of this analysis, the constraint configured in the FEM simulation program is equivalent to an embedding (fixed geometry) in the same region of the connection. Especially in this simulation, 75,000 nodes, 53,252 elements and 224,739 DOF (degrees of freedom) were used. Table 1 presents frequencies measured at 5 K (experimental values), frequencies obtained through simulation without considering the action of gravity, and frequencies obtained through simulation considering the effect of gravity.

Table 1. Experimentally captured frequency values [16] (left column) and frequency values through simulation without considering the effect of gravity (middle column) and considering the effect of gravity (right column), the latter two used in this work .

Measured Frequency (Hz) [16]	Simulated frequency (Hz)	Simulated frequency (GRAV) (Hz)
3,172.5	3,173.6	3,183.2
3,183.0	3,173.7	3,183.3
3,213.6	3,193.4	3,200.3
3,222.0	3,193.4	3,200.4
3,240.0	3,208.6	3,212.4
Bandwidth = 67.5 Hz	Bandwidth = 35.0 Hz	Bandwidth= 29.2 Hz

6. Conclusion

When analyzing the effect of the action of gravity on the results obtained through simulation by FEM for the modal frequencies of the Schenberg antenna, an increase in the frequency values was noticed, as well as an alteration in its band. It was also noticed that the increase in frequency was greater for doublets with less frequency. However, these changes were expected due to the effect of internal voltages on these frequencies, an effect that was not considered before.

When comparing the values simulated under the action of gravity with the values obtained experimentally, it is clear that the model used still needs to be improved. This conclusion is obtained by observing the difference between the experimental and simulated values for the frequencies, as well as the significant difference between the respective bands.

Acknowledgments
CF acknowledges FAPESP (Brazil) for grants #2013/26258-4 and #2006/56041-3 as well as CNPq for grant 309098/2017-3.

References

[1] Frajuca C *et al* 2020 *Journal of Physics: Conference Series* **1730** 012025
[2] Fabricio Junior C A *et al* 2020 *Journal of Physics: Conference Series* **1730** 012082
[3] Aguiar O D *et al.* 2006 *Journal Class. Quantum Grav.* **23**, 239
[4] Frajuca C *et al.* 2004 *Class. Quantum Grav.* **21** 1107
[5] Velloso W F, Aguiar OD and Magalhaes NS *Proc. First International Workshop for an Omnidirectional Gravitational Radiation Observatory* 1997 Singapore:World Scientific
[6] Magalhaes N S *et al.* 1997 *Astrophysical Journal* **475**, 462
[7] Magalhaes N S *et al.* 1995 *MNRAS* **274**, 670
[8] Magalhaes N S *et al* 1997 *Gen. Relat. Grav.* **29** 1511
[9] Aguiar O D et. al. 2005 *Class. Quantum Grav.* **22**, 209
[10] Frajuca *et al* 2002 *Class. Quantum Grav.* **19** 1961
[11] Ribeiro K L *et al.* 2004 *Class. Quantum Grav.* **21,** 1225
[12] Aguiar O D et al. 2012 *Journal of Physics: Conference Series* **363,** 012003
[13] Van Albada *et al* 2000 *Review of Scientific Instruments* **71** 1345
[14] Frajuca C, Bortoli F S, Magalhaes N S 2005 *Brazilian Journal of Physics* **35** 1201
[15] Frajuca C, Bortoli F S, Magalhaes N S 2006 *Journal of Physics: Conference Series* **32** 319
[16] Aguiar O D et al. 2004 *Class. Quantum Grav.* **21** 459
[17] Bortoli F S *et al* 2010 *Journal of Physics: Conference Series* **228** 012011.
[18] Andrade L A *et al.* 2004 *Class. Quantum Grav.* **21,** 1215
[19] Aguiar O D *et al 2002 Brazilian Journal of Physics* **32** 866
[20] Bortoli F S *et al* 2019 *Brazilian Journal of Physic* **49** 133
[21] Frajuca C, Bortoli F S, Magalhaes N S, Horiguti A M 2008 *Journal of Physics: Conference Series* **122** 012029
[22] Magalhaes N S, Miranda T A, Frajuca C 2012 *Astrophysical Journal* **755**, 54[26] Frajuca C, Bortoli F S 2006 *Journal of Physics: Conference Series* **32** 315
[23] Bortoli F S *et al* 2016 *Brazilian Journal of Physic* **46** 308
[24] Frajuca C *et al.* 2018 *Journal of the Brazilian Society of Mechanical Sciences and Engineering* **40** 319
[25] Bortoli F S *et al* 2020 *Brazilian Journal of Physic* **50** 541
[26] Aguiar O D *et al* 2002 The Ninth Marcel Grossmann Meeting: On Recent Developments in Theoretical and Experimental General Relativity, Gravitation and Relativistic Field Theories 1891
[27] Frajuca C, Bortoli F S 2019 *Journal of Physics:Conference Series* **1391** 012029
[28] Merkowitz S M 1998 *Physical Review D* **58** 062002